Rapid Communications

Atomic-orbital-free intrinsic ferromagnetism in electrenes

Jun Zhou [1,*] Yuan Ping Feng [1,2,†] and Lei Shen (沈雷) [3,4,‡]

[1]*Department of Physics, National University of Singapore, Singapore 117551*
[2]*Center for Advanced 2D Materials, National University of Singapore, Singapore 117546*
[3]*Department of Mechanical Engineering, National University of Singapore, Singapore 117575*
[4]*Engineering Science Programme, National University of Singapore, Singapore 117575*

(Received 8 April 2019; revised 26 October 2020; accepted 29 October 2020; published 17 November 2020)

Atomic orbitals play fundamental roles in the modern theory of magnetism, not only providing local moments via their partial occupation, but also offering exchange interactions through their direct or indirect hybridization. Here, we report atomic-orbital-free intrinsic ferromagnetism in monolayer electrides or electrenes, in which excess electrons act as anions. Taking the honeycomb $LaBr_2$ ($La^{3+}Br_2^- \cdot e^-$) as an example, our first-principles calculations, in combination with a low-energy effective model in the basis of the Wannier function and Anderson's superexchange theory, reveal that the excess electron is localized at the center of the hexagon, which leads to the spontaneous formation of a local moment due to the strong Stoner instability of the associated state near the Fermi level (E_f). The large off-site Coulomb interaction and extended tails of both wave and Wannier functions indicate a significant spatial extension of the anionic electron state in $LaBr_2$. The overlap of the long tails mediates an extended ferromagnetic direct exchange to second-nearest neighbors (up to 7–8 Å), in sharp contrast to the conventional direct exchange which is short ranged due to the overlap of atomic orbitals with limited spatial extension. The dual nature, localization and extension, of the anionic electron state results in a unique magnetic mechanism in such atomic-orbital-free intrinsic two-dimensional ferromagnets.

DOI: 10.1103/PhysRevB.102.180407

Introduction. Ferromagnetism (FM) in two-dimensional (2D) materials has been a hot research topic, because such materials offer special advantages of high data storage density and easy integration into semiconductor devices [1]. Recently, Gong *et al.* [2] and Huang *et al.* [3] first succeeded in fabricating intrinsic 2D ferromagnets, $Cr_2Ge_2Te_6$ and CrI_3 respectively, demonstrating the possibility of fabricating robust 2D intrinsic ferromagnets. Quickly, more intrinsic 2D ferromagnets, including Fe_3GeTe_2 [4], VSe_2 [5], CrOBr [6], CrSeBr [7], $CrWGe_2Te_6$ [8], $MnPSe_3$ [9], CoH_2 [10], and $CrBr_3$ [11] were reported. It is noted that the magnetism in these intrinsic 2D magnetic materials can be understood by the conventional theory of magnetism developed for 3D magnetic materials. For example, the formation of local magnetic moments in FM semiconductors $Cr_2Ge_2Te_6$ and CrI_3 is associated with the magnetic element Cr, which has partially filled 3*d* orbitals. The strongly localized nature of the 3*d* states under the crystal field favors spontaneous spin polarization and leads to the formation of local moments. These local moments are coupled via the 5*p* orbital of Te or I, by the superexchange within the Goodenough-Kanamori-Anderson (GKA) rules [12]. For ferromagnetic systems with free electrons, such as FM metals Fe_3GeTe_2 or VSe_2, the itinerary carriers can mediate a long-range indirect exchange between the local moments within the 3*d* orbitals via the Ruderman-Kittel-Kasuya-Yosida (RKKY) or Zener double exchange [13,14]. As can be seen, atomic orbitals play an essential role in conventional magnetic materials. Without them, there would be neither local moments of spin-polarized electrons nor exchange interactions through direct or indirect orbital hybridization.

In a family of intrinsic electron-rich materials, electrides or electrenes in 2D, excess electrons (named anionic electrons) are confined in geometrically interstitial sites and do not occupy any atomic orbital, acting as anions [15]. Such anionic electrons are loosely bounded and demonstrate some unique physical properties, such as superconductivity [16,17], topological matters [18–21], and Dirac plasmons [22]. Given the unique feature of the anionic electron state in electrenes and the enormous interest in 2D intrinsic ferromagnetic materials, it is natural to ask whether electrenes can be a new type of intrinsic 2D magnetic system. With such a motivation, we screened more than 6000 structures in the 2D materials database 2DMatPedia [23] for magnetic electrenes. Our search resulted in nine magnetic electrenes, and to our surprise, four of them ($LaBr_2$, La_2Br_5, Sc_7Cl_{10}, and Ba_2LiN) contain no magnetic elements [24]. A question then arises: What is the origin of magnetism in such electrenes without magnetic elements?

In this Rapid Communication, taking $LaBr_2$ as an example, we demonstrate the intrinsic atomic-orbital-free magnetism in this group of 2D materials. The results of our first-principles calculations using the density functional theory (DFT) indicate that the excess electron in $LaBr_2$ does not occupy any atomic orbital but localizes at the center of the hexagon of

*phyzjun@nus.edu.sg
†phyfyp@nus.edu.sg
‡shenlei@nus.edu.sg

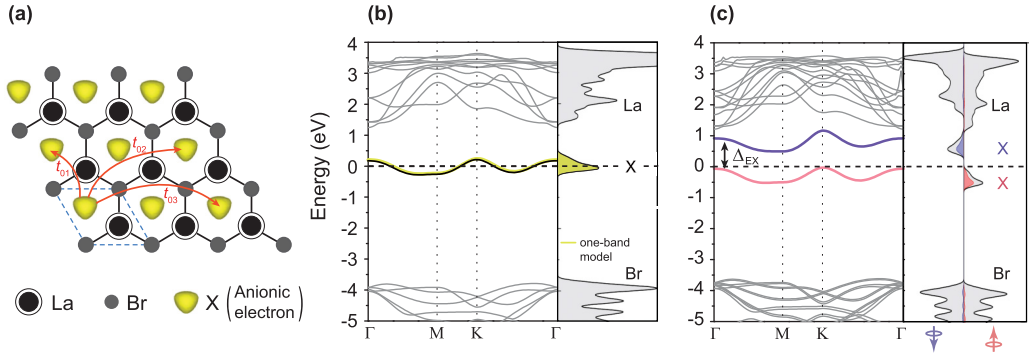

FIG. 1. (a) $LaBr_2$ ($La^{3+}Br_2^- \cdot e^-$) ML in the H-phase MoS_2 structure with ELF maps (isosurface value = 0.75) in yellow. The dashed diamond denotes the unit cell. Only the ELF on interstitial sites is shown for clarity. The anionic electron in the geometric space, labeled as X, is at the center of each hexagon. The red arrows are the schematic representation of the hopping paths between anionic electrons, and the calculated hopping parameters are $t_{01} = 12.50$ meV, $t_{02} = 53.18$ meV, and $t_{03} = -9.11$ meV, respectively. Band structure and density of states of ML $LaBr_2$ (b) without and (c) with spin polarization. The yellow band and DOS in (b) are from the one-band tight-binding model.

its honeycomb hexagonal crystal structure [see details and justification of the calculation methodologies based on VASP, Wannier function, constrained random phase approximation (cRPA), and Monte Carlo simulations in the Supplemental Material (SM) [25] (see also Refs. [26–42] therein)]. Each anionic electron carries a magnetic moment of $1\mu_B$, which corresponds to the $s = 1/2$ interstitial state characterized by a half-filled band near the Fermi level. The underlying physics of the magnetic exchange interaction is further understood by a low-energy effective model, in which the parameters are mapped from the Wannier functions by the cRPA. We show that while the localization of the anionic electron state induces the magnetic moment, the strong overlap of the spatially extended tails of the wave and Wannier functions results in a direct-exchange interaction over an extended range to the second-nearest neighbors (up to 7–8 Å). This is in sharp contrast to the *conventional* direct exchange in magnetic materials which is very short ranged due to the limited spatial extension of the atomic orbitals.

Structure of monolayer $LaBr_2$. Layered bulk $LaBr_2$ was synthesized experimentally in 1989 [43]. Its crystal structure resembles that of the 2H phase of MoS_2 (space group $P6_3/mmc$) as shown in Fig. 1(a). The excess electron in $La^{3+}Br_2^- \cdot e^-$, as an ion, is confined in the center of the hexagon and is free from any atomic orbitals [Fig. 1(a)]. The calculated exfoliation energy of $LaBr_2$ is 0.27 J/m^2 which is lower than that of Ca_2N (1.13 J/m^2) [44] and graphene (0.43 J/m^2) [45]. This indicates that monolayer (ML) $LaBr_2$ can be exfoliated from bulk $LaBr_2$, similar to how electrene Ca_2N is isolated experimentally from its bulk counterpart by liquid exfoliation [46]. Furthermore, both the calculated phonon spectrum and *ab initio* molecular dynamics simulation confirm the thermodynamic structural stability of ML $LaBr_2$ [47,48].

Origin of local moments. In conventional magnetic materials, the formation of local moments is associated with partially filled atomic orbitals [3,4]. Their strongly localized nature favors spin polarization and leads to the formation of local moments. However, the magnetic moments in ML $LaBr_2$ are of a different nature. As shown in Fig. 1(b), there is a narrow band near the Fermi level, which is mainly from the anionic electrons labeled as X in Fig. 1(a). According to the Stoner criterion, $g(E_f)I > 1$, where $g(E_f)$ is the density of states (DOS) at E_f and I denotes the Stoner parameter [49], this strongly localized state of the interstitial electron is unstable and would lead to spontaneous spin polarization. The electronic structure of ML $LaBr_2$ calculated with the spin polarization [Fig. 1(c)] shows a local moment of $1\mu_B$ per unit cell (u.c.). The spin-exchange splitting energy (Δ_{EX}) is around 1 eV, comparable to that of the Mn_{3d} orbital (1.62 eV) for $M = 2\mu_B$ [50]. The calculated electron localization function (ELF), projected DOS, and spin density all confirm that the magnetic moment is mainly contributed by the atomic-orbital-free anionic electron localized at a geometrically interstitial region [25].

Mechanism of ferromagnetic exchange. It is known that the magnetic exchange between the local moments, either directly or indirectly, plays a key role in determining the magnetic properties, such as ferromagnetism or antiferromagnetism (AFM). The conventional direct exchange due to the direct overlap of atomic orbitals is usually short ranged. The range of interaction can be extended in *d-p-d* superexchange, *p-d* exchange, and *s-f* RKKY [13,14,51–53]. Nevertheless, all these interactions are based on atomic orbitals and none of these magnetic exchange models is applicable to the *atomic-orbital-free* magnetism in $LaBr_2$.

In order to understand the coupling between the magnetic anionic electrons, we examine the nature of the anionic electron state. In Fig. 2(a), we compare the radial distributions of the wave functions of the anionic electron state and the Cr_{3d} and I_{5p} orbitals in CrI_3 which is a well-known 2D ferromagnetic material [3]. It is found that the state of the anionic electron is almost as localized as the atomic d state, and meanwhile is more extended than the atomic p state. Based on this duality (localization and extension) of the anionic electron state, we propose that the formation of the local moment is from the localized feature, while the ferromagnetic interaction between the atomic-orbital-free anionic electrons in ML $LaBr_2$ is mediated by an overlap of the extended anionic electron state, as illustrated in Fig. 2(b). Based on this mechanism, the weakening of either the localization or the extension of the anionic electron state is expected to reduce the magnetism. For example, applying an in-plane biaxial tensile strain of

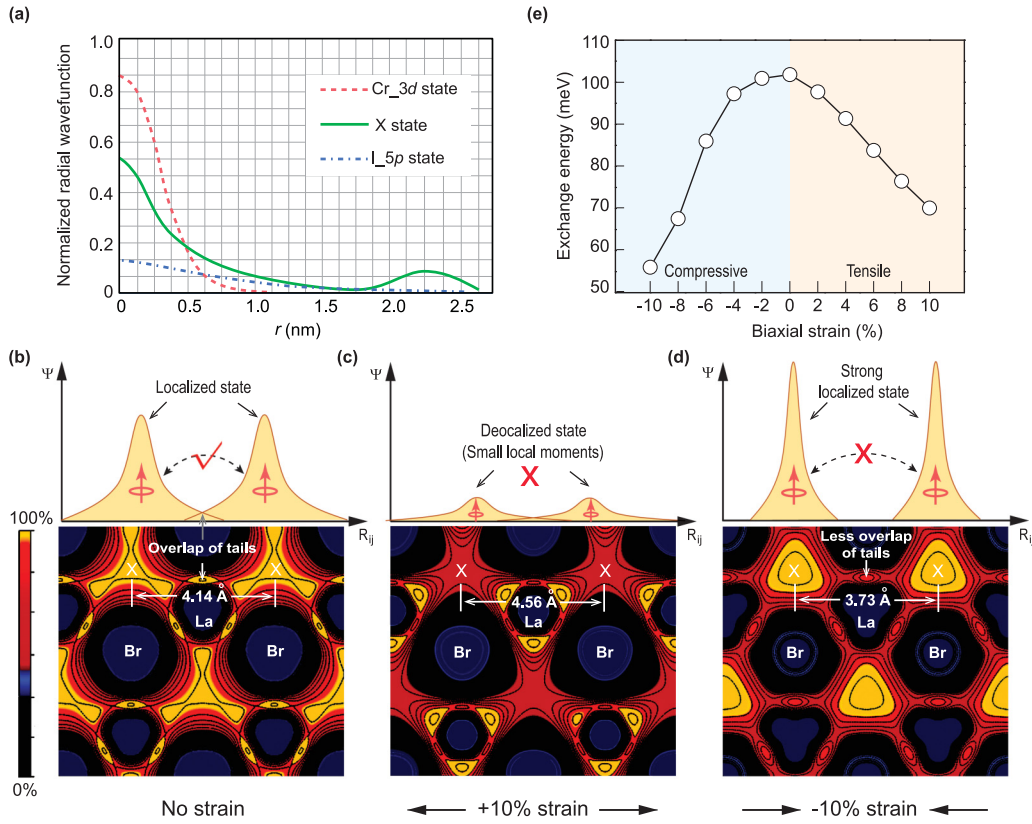

FIG. 2. (a) Radial distributions of the normalized wave function of states of Cr_{3d}, I_{5p}, and the anionic electron. Schematics of strain-induced changes in the localization of wave functions and their overlap (upper panel) as well as the calculated spin density (lower panel) of (b) strain-free ML $LaBr_2$, (c) ML $LaBr_2$ with 10% tensile strain, and (d) ML $LaBr_2$ with 10% compressive strain. The isovalue is $0.001e/Å^3$. (e) The strain dependence of the exchange energy, which is calculated by the total energy difference between the AFM and FM configurations.

10% leads to a decrease of local moments, while an in-plane biaxial compressive strain of 10% reduces the overlap between the tails of the wave functions, as shown in Figs. 2(c) and 2(d), respectively, both resulting in a weaker exchange interaction compared with the undeformed structure, as shown in Fig. 2(e).

Low-energy effective model. While the DFT results above have clearly shown the unique dual nature of the atomic-orbital-free magnetic state of the anionic electron in $LaBr_2$, we construct a low-energy effective model in terms of the Wannier function associated with the interstitial state of the anionic electron to further understand the underlying mechanism. It is because this model allows us to explicitly include the Coulomb interaction on the nonatomic interstitial site and nonlocal direct exchange interaction. We adopt the one-orbital extended Hubbard model in which the Hamiltonian of the system based on the second quantization is given by [54,55]

$$\hat{H} = \sum_{ij,\sigma\sigma'} t_{ij}^{\sigma\sigma'} \hat{\alpha}_{i\sigma}^{\dagger} \hat{\alpha}_{j\sigma'} + \frac{1}{2} \sum_{i,\sigma\sigma'} U_{00} \hat{\alpha}_{i\sigma}^{\dagger} \hat{\alpha}_{i\sigma'}^{\dagger} \hat{\alpha}_{i\sigma'} \hat{\alpha}_{i\sigma} + \frac{1}{2} \sum_{ij,\sigma\sigma'} U_{ij} \hat{\alpha}_{i\sigma}^{\dagger} \hat{\alpha}_{j\sigma'}^{\dagger} \hat{\alpha}_{j\sigma'} \hat{\alpha}_{i\sigma} + \frac{1}{2} \sum_{ij,\sigma\sigma'} J_{ij}^{D} \hat{\alpha}_{i\sigma}^{\dagger} \hat{\alpha}_{j\sigma'}^{\dagger} \hat{\alpha}_{i\sigma'} \hat{\alpha}_{j\sigma}, \tag{1}$$

where $i(j)$ and $\sigma(\sigma')$ are site and spin indices; $\hat{\alpha}_{i\sigma}^{\dagger}(\hat{\alpha}_{i\sigma})$ are the creation (annihilation) operators and $t_{ij}^{\sigma\sigma'}$, U_{00}, U_{ij}, and J_{ij}^{D} are the hopping parameters, on-site Coulomb, off-site Coulomb, and off-site direct-exchange interactions, respectively.

To map the parameters in this model, we construct a maximally localized Wannier function (MLWF) for the band of the anionic electron near E_f using the WANNIER90 package [56]. The hopping parameters $t_{ij}^{\sigma\sigma'}$ were obtained via the Wannier parametrization [56,57]. Based on the constructed MLWF, we then extract the partially screened U_{00}, U_{ij}, and J_{ij}^{D} using cRPA as implemented in VASP, excluding the "self-screening" transition for the band of the anionic electron (see details in SM [25]). Different MLWFs are constructed and the interstitial-centered MLWF is found to best describe the anionic electron state [25], which captures the extended tails around the well-localized *s*-symmetric body, as shown in the colored contour plot in the plane passing through the La atoms [Figs. 3(a) and 3(b)].

The cRPA based on this MLWF yields $t_{01} = 12.50$ meV, $U_{00} = 2.32$ eV, $U_{01} = 1.36$ eV, $J_{01}^{D} = 21.9$ meV, and $J_{02}^{D} = 1.9$ meV. It is surprising that direct-exchange coupling remains significant between the second-nearest neighbors over 7.17 Å in $LaBr_2$, which is much longer than any atomic orbital. Furthermore, the strength of the off-site Coulomb interaction U_{01} is quite large (~60% of U_{00}), which indicates a significant spatial charge fluctuation in $LaBr_2$, in line with the extended nature of the anionic electron. The large U_{00} and U_{01} are the results of the weak screening from the atomic states

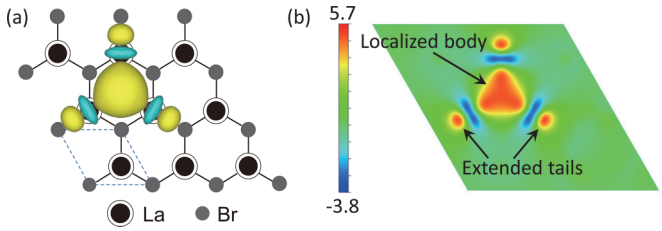

FIG. 3. The maximally localized Wannier function (a) and its colored contour plot in the plane passing through the La atoms (b) of the anionic electron state of $LaBr_2$. The isovalue of MLWF is set to 2.0. The localized *s*-symmetric body and its extended tails of Wannier function are indicated by black arrows.

as the anionic electron state near E_f is well isolated from other bands. It is remarkable that the anionic electron state in $LaBr_2$ has a significant spatial extension and overlaps in a long distance, leading to an extended direct-exchange interaction J_{ij}^D. This atomic-orbital-free direct exchange goes beyond the spatial limit of atomic-orbital overlap in other direct-exchange systems. It is noted that the effective Coulomb interaction $\tilde{U} = U_{00} - U_{01}$ of $LaBr_2$ is much larger than the hopping integral ($\tilde{U} \sim 77t_{01}$), which is within the range of a magnetic insulating phase on the triangular lattice [58,59], consistent with the localized nature of the anionic electron.

In the limit of $U \gg t_{01}$, the overall isotropic exchange interaction of $LaBr_2$ can be described by the magnetic Anderson's model as follows [60],

$$J_{ij} = \frac{1}{\tilde{U}} Tr_\sigma \{\hat{t}_{ji}\hat{t}_{ij}\} - J_{ij}^D, \tag{2}$$

where the first term is the antiferromagnetic superexchange from direct hopping between magnetic centers while the second term is the ferromagnetic direct exchange from the overlap of the wave functions of magnetic moments. Using the parameters obtained from Eq. (1), the nearest-neighboring kinetic AFM superexchange and direct FM exchange is 0.2 and 21.9 meV, respectively, and the overall isotropic exchange energy is -21.7 meV for $LaBr_2$. This isotropic exchange is stronger than the DFT result (-6.5 meV) because the latter is known for its inadequacy in describing the nonlocal direct-exchange interaction [61], justifying the rational choice of the low-energy effective model in unveiling the underlying exchange mechanism of atomic-orbital-free intrinsic magnetism in electrenes.

Possible magnetic enhancement. The trend of magnetic stability of $LaBr_2$ and its possible enhancement are studied by Monte Carlo (MC) simulations [62,63]. The calculated Curie temperature (T_c) and coercive field (H_c) are 235 K and 0.53 T, respectively, for pristine $LaBr_2$ (see Fig. 4). Since many experiments have demonstrated an increase of the Curie temperature of 2D FM semiconductors by charge doping [4,64,65], we perform calculations at different charge doping levels. The inset in Fig. 4(a) shows the dependence of the exchange energy on the doping concentration which is varied from $-0.02e$ (electron doping) to $+0.1e$ (hole doping) per unit cell. Results of our MC simulation indicate that $0.1e$/u.c. hole doping increased both the T_c (341 K) and the H_c (0.71 T). Charge doping can be easily achieved experimentally by applying an external electric field [4,64,65]. This trend is in qualitative agreement with a recent experimental observation that hole doping increases both T_c and H_c of CrI_3 [64].

Conclusion. In conclusion, another type of 2D intrinsic ferromagnetic material, electrenes, with *atomic-orbital-free* magnetism is proposed. The physical origin of the local moments and magnetic exchange interactions in monolayer $LaBr_2$ is thoroughly investigated by the first-principles calculations, low-energy effective model, and magnetic Anderson's model. The anionic electron is localized but has significantly extended tails. The localized nature results in spin polarization and the formation of local moments. The overlap of its extended tails, on the other hand, promotes a direct-exchange interaction over an extended distance beyond the conventional direct exchange.

Finally, we wish to point out that we have taken $LaBr_2$, a layered electride, as an example to demonstrate the concept of anionic electron-induced ferromagnetic order. However,

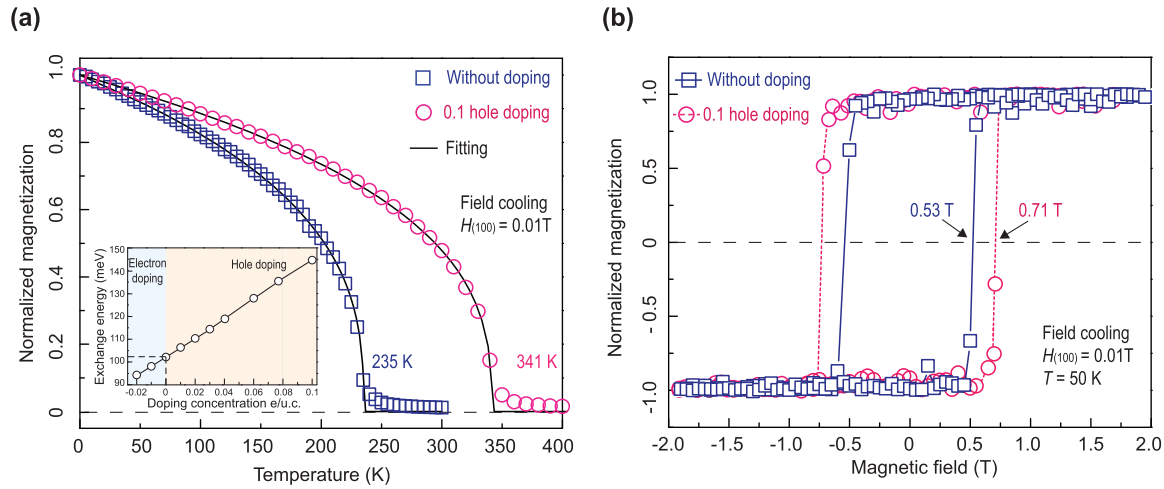

FIG. 4. (a) The temperature dependence of magnetization without (square) and with (circle) $0.1e$/u.c. hole doping. A cooling field of 0.01 T is applied along the (100) direction. The inset shows the doping concentration dependence of the exchange energy. (b) The simulated magnetic field dependence of magnetization at the temperature of 50 K.

electrides are a big family [18,19,24,66,67]. The physical mechanism proposed in this Rapid Communication can be applied to ferromagnetism in other FM electrides. As reminded by Eick 30 years ago [68], they are "still a veritable gold mine" that are worthy of further studies on these intrinsic electron-rich materials which may have intriguing properties and unique technological applications. For example, very recently, Liu *et al.* reported an intrinsic quantum anomalous Hall effect induced by in-plane magnetization in LaCl [20,21]. Hirayama *et al.* proposed a class of electrides with exotic topological properties [19]. We hope this work will stimulate further experimental and theoretical studies to discover more magnetic electrenes and explore the spin physics in these types of 2D intrinsic magnetic systems, which may lead to practical spintronic applications.

Note added in proof. Recently, we became aware of a similar work by Badrtdinov and Nikolaev [69]. They investigated two of the four intrinsic ferromagnetic electrenes proposed in our work by similar theoretical approaches, uncovering the dual localized and extended nature of anionic electrons in magnetic electrenes.

Acknowledgments. This work was supported by the Singapore Ministry of Education Academic Research Fund Tier 1 Grants No. R-144-000-361-112, No. R-144-000-413-114, No. R-265-000-615-114, No. R-265-000-651-114, and No. R265-000-691-114. The authors thank Dr. Vladimir Mazurenko for his help in calculating the local and nonlocal Coulomb interactions. We thank Dr. Lei Xu and Dr. Tao Zhu for their calculation and discussion on Wannier functions and constrained random phase approximation (cRPA). We thank Dr. Xiao Wang, Dr. Shengyuan Yang, and Dr. Yongzheng Luo for their helpful discussions. The calculations were carried out on the CA2DM-NUS and National Supercomputing Centre Singapore high-performance computing facilities.

[1] Y. P. Feng, L. Shen, M. Yang, A. Wang, M. Zeng, Q. Wu, S. Chintalapati, and C.-R. Chang, Prospects of spintronics based on 2D materials, Wiley Interdiscip. Rev. Comput. Mol. Sci. **7**, e1313 (2017).

[2] C. Gong, L. Li, Z. Li, H. Ji, A. Stern, Y. Xia, T. Cao, W. Bao, C. Wang, Y. Wang *et al.*, Discovery of intrinsic ferromagnetism in two-dimensional van der Waals crystals, Nature (London) **546**, 265 (2017).

[3] B. Huang, G. Clark, E. Navarro-Moratalla, D. R. Klein, R. Cheng, K. L. Seyler, D. Zhong, E. Schmidgall, M. A. McGuire, D. H. Cobden *et al.*, Layer-dependent ferromagnetism in a van der Waals crystal down to the monolayer limit, Nature (London) **546**, 270 (2017).

[4] Y. Deng, Y. Yu, Y. Song, J. Zhang, N. Z. Wang, Z. Sun, Y. Yi, Y. Z. Wu, S. Wu, J. Zhu *et al.*, Gate-tunable room-temperature ferromagnetism in two-dimensional Fe_3GeTe_2, Nature (London) **563**, 94 (2018).

[5] M. Bonilla, S. Kolekar, Y. Ma, H. C. Diaz, V. Kalappattil, R. Das, T. Eggers, H. R. Gutierrez, M.-H. Phan, and M. Batzill, Strong room-temperature ferromagnetism in VSe_2 monolayers on van der Waals substrates, Nat. Nanotechnol. **13**, 289 (2018).

[6] N. Miao, B. Xu, L. Zhu, J. Zhou, and Z. Sun, 2D intrinsic ferromagnets from van der Waals antiferromagnets, J. Am. Chem. Soc. **140**, 2417 (2018).

[7] Z. Jiang, P. Wang, J. Xing, X. Jiang, and J. Zhao, Screening and design of novel 2D ferromagnetic materials with high Curie temperature above room temperature, ACS Appl. Mater. Interfaces **10**, 39032 (2018).

[8] C. Huang, J. Feng, F. Wu, D. Ahmed, B. Huang, H. Xiang, K. Deng, and E. Kan, Toward intrinsic room-temperature ferromagnetism in two-dimensional semiconductors, J. Am. Chem. Soc. **140**, 11519 (2018).

[9] X. Li, X. Wu, and J. Yang, Half-metallicity in $MnPSe_3$ exfoliated nanosheet with carrier doping, J. Am. Chem. Soc. **136**, 11065 (2014).

[10] Q. Wu, Y. Zhang, Q. Zhou, J. Wang, and X. C. Zeng, Transition-metal dihydride monolayers: A new family of two-dimensional ferromagnetic materials with intrinsic room-temperature half-metallicity, J. Phys. Chem. Lett. **9**, 4260 (2018).

[11] C. Huang, Y. Du, H. Wu, H. Xiang, K. Deng, and E. Kan, Prediction of Intrinsic Ferromagnetic Ferroelectricity in a Transition-Metal Halide Monolayer, Phys. Rev. Lett. **120**, 147601 (2018).

[12] P. W. Anderson, Antiferromagnetism. Theory of superexchange interaction, Phys. Rev. **79**, 350 (1950).

[13] M. A. Ruderman and C. Kittel, Indirect exchange coupling of nuclear magnetic moments by conduction electrons, Phys. Rev. **96**, 99 (1954).

[14] C. Zener, Interaction between the d-shells in the transition metals. II. Ferromagnetic compounds of manganese with perovskite structure, Phys. Rev. **82**, 403 (1951).

[15] J. L. Dye, Electrons as anions, Science **301**, 607 (2003).

[16] Y. Zhang, B. Wang, Z. Xiao, Y. Lu, T. Kamiya, Y. Uwatoko, H. Kageyama, and H. Hosono, Electride and superconductivity behaviors in Mn_5Si_3-type intermetallics, npj Quantum Mater. **2**, 45 (2017).

[17] Z. Zhao, S. Zhang, T. Yu, H. Xu, A. Bergara, and G. Yang, Predicted Pressure-Induced Superconducting Transition in Electride Li_6P, Phys. Rev. Lett. **122**, 097002 (2019).

[18] C. Park, S. W. Kim, and M. Yoon, First-Principles Prediction of New Electrides with Nontrivial Band Topology Based on One-Dimensional Building Blocks, Phys. Rev. Lett. **120**, 026401 (2018).

[19] M. Hirayama, S. Matsuishi, H. Hosono, and S. Murakami, Electrides as a New Platform of Topological Materials, Phys. Rev. X **8**, 031067 (2018).

[20] H. Huang, K.-H. Jin, S. Zhang, and F. Liu, Topological electride Y_2C, Nano. Lett. **18**, 1972 (2018).

[21] Z. Liu, G. Zhao, B. Liu, Z. F. Wang, J. Yang, and F. Liu, Intrinsic Quantum Anomalous Hall Effect with in-Plane Magnetization: Searching Rule and Material Prediction, Phys. Rev. Lett. **121**, 246401 (2018).

[22] J. Wang, X. Sui, S. Gao, W. Duan, F. Liu, and B. Huang, Anomalous Dirac Plasmons in 1D Topological Electrides, Phys. Rev. Lett. **123**, 206402 (2019).

[23] J. Zhou, L. Shen, M. D. Costa, K. A. Persson, S. P. Ong, P. Huck, Y. Lu, X. Ma, Y. Chen, H. Tang *et al.*, 2DMatPedia, an open computational database of two-dimensional materials

from top-down and bottom-up approaches, Sci. Data **6**, 86 (2019); http://www.2dmatpedia.org/.

[24] J. Zhou, L. Shen, M. Yang, H. Cheng, W. Kong, and Y. P. Feng, Discovery of hidden classes of layered electrides by extensive high-throughput material screening, Chem. Mater. **31**, 1860 (2019).

[25] See Supplemental Material at http://link.aps.org/supplemental/10.1103/PhysRevB.102.180407 for details and validation of computational methodologies, as well as more DFT results.

[26] G. Kresse and J. Hafner, *Ab initio* molecular dynamics for liquid metals, Phys. Rev. B **47**, 558 (1993).

[27] G. Kresse and J. Hafner, *Ab initio* molecular-dynamics simulation of the liquid-metal–amorphous-semiconductor transition in germanium, Phys. Rev. B **49**, 14251 (1994).

[28] G. Kresse and D. Joubert, From ultrasoft pseudopotentials to the projector augmented-wave method, Phys. Rev. B **59**, 1758 (1999).

[29] J. Hubbard, Electron correlations in narrow energy bands, Proc. R. Soc. London, Ser. A **276**, 238 (1963).

[30] S. L. Dudarev, G. A. Botton, S. Y. Savrasov, C. J. Humphreys, and A. P. Sutton, Electron-energy-loss spectra and the structural stability of nickel oxide: An LSDA+U study, Phys. Rev. B **57**, 1505 (1998).

[31] M. Topsakal and R. M. Wentzcovitch, Accurate projected augmented wave (PAW) datasets for rare-earth elements (RE = La–Lu), Comput. Mater. Sci. **95**, 263 (2014).

[32] M. Dion, H. Rydberg, E. Schröder, D. C. Langreth, and B. I. Lundqvist, Van der Waals Density Functional for General Geometries, Phys. Rev. Lett. **92**, 246401 (2004).

[33] J. Klimeš, D. R. Bowler, and A. Michaelides, Chemical accuracy for the van der Waals density functional, J. Phys.: Condens. Matter **22**, 022201 (2009).

[34] G. Román-Pérez and J. M. Soler, Efficient Implementation of a van der Waals Density Functional: Application to Double-Wall Carbon Nanotubes, Phys. Rev. Lett. **103**, 096102 (2009).

[35] J. Klimes, D. R. Bowler, and A. Michaelides, Van der Waals density functionals applied to solids, Phys. Rev. B **83**, 195131 (2011).

[36] A. A. Mostofi, J. R. Yates, Y.-S. Lee, I. Souza, D. Vanderbilt, and N. Marzari, WANNIER90: A tool for obtaining maximally-localised Wannier functions, Comput. Phys. Commun. **178**, 685 (2008).

[37] C. Edmiston and K. Ruedenberg, Localized atomic and molecular orbitals, Rev. Mod. Phys. **35**, 457 (1963).

[38] C. L. Gao, W. Wulfhekel, and J. Kirschner, Revealing the 120° Antiferromagnetic Néel Structure in Real Space: One Monolayer Mn on Ag(111), Phys. Rev. Lett. **101**, 267205 (2008).

[39] W.-B. Zhang, Q. Qu, P. Zhu, and C.-H. Lam, Robust intrinsic ferromagnetism and half semiconductivity in stable two-dimensional single-layer chromium trihalides, J. Mater. Chem. C **3**, 12457 (2015).

[40] H.-R. Fuh, C.-R. Chang, Y.-K. Wang, R. F. Evans, R. W. Chantrell, and H.-T. Jeng, Newtype single-layer magnetic semiconductor in transition-metal dichalcogenides VX_2 (X = S, Se and Te), Sci. Rep. **6**, 32625 (2016).

[41] X. Li and J. Yang, $CrXTe_3$ (X = Si, Ge) nanosheets: two dimensional intrinsic ferromagnetic semiconductors, J. Mater. Chem. C **2**, 7071 (2014).

[42] R. F. L. Evans, U. Atxitia, and R. W. Chantrell, Quantitative simulation of temperature-dependent magnetization dynamics and equilibrium properties of elemental ferromagnets, Phys. Rev. B **91**, 144425 (2015).

[43] K. Kramer, T. Schleid, M. Schulze, W. Urland, and G. Meyer, Three bromides of lanthanum: $LaBr_2$, La_2Br_5, and $LaBr_3$, Z. Anorg. Allg. Chem. **575**, 61 (1989).

[44] S. Zhao, Z. Li, and J. Yang, Obtaining two-dimensional electron gas in free space without resorting to electron doping: An electride based design, J. Am. Chem. Soc. **136**, 13313 (2014).

[45] R. Zacharia, H. Ulbricht, and T. Hertel, Interlayer cohesive energy of graphite from thermal desorption of polyaromatic hydrocarbons, Phys. Rev. B **69**, 155406 (2004).

[46] D. L. Druffel, K. L. Kuntz, A. H. Woomer, F. M. Alcorn, J. Hu, C. L. Donley, and S. C. Warren, Experimental demonstration of an electride as a 2D material, J. Am. Chem. Soc. **138**, 16089 (2016).

[47] A. Togo and I. Tanaka, First principles phonon calculations in materials science, Scr. Mater. **108**, 1 (2015).

[48] S. Nosé, A unified formulation of the constant temperature molecular dynamics methods, J. Chem. Phys. **81**, 511 (1984).

[49] E. C. Stoner, Collective electron ferromagnetism, Proc. R. Soc. London A **165**, 372 (1938).

[50] H. Peng, H. J. Xiang, S.-H. Wei, S.-S. Li, J.-B. Xia, and J. Li, Origin and Enhancement of Hole-Induced Ferromagnetism in First-Row d^0 Semiconductors, Phys. Rev. Lett. **102**, 017201 (2009).

[51] H. Pan, J. B. Yi, L. Shen, R. Q. Wu, J. H. Yang, J. Y. Lin, Y. P. Feng, J. Ding, L. H. Van, and J. H. Yin, Room-Temperature Ferromagnetism in Carbon-Doped ZnO, Phys. Rev. Lett. **99**, 127201 (2007).

[52] L. Shen, R. Q. Wu, H. Pan, G. W. Peng, M. Yang, Z. D. Sha, and Y. P. Feng, Mechanism of ferromagnetism in nitrogen-doped ZnO: First-principle calculations, Phys. Rev. B **78**, 073306 (2008).

[53] L. Shen, M. Zeng, Y. Lu, M. Yang, and Y. P. Feng, Simultaneous Magnetic and Charge Doping of Topological Insulators with Carbon, Phys. Rev. Lett. **111**, 236803 (2013).

[54] I. V. Solovyev, Z. V. Pchelkina, and V. V. Mazurenko, Magnetism of sodium superoxide, CrystEngComm **16**, 522 (2014).

[55] V. V. Mazurenko, A. N. Rudenko, S. A. Nikolaev, D. S. Medvedeva, A. I. Lichtenstein, and M. I. Katsnelson, Role of direct exchange and Dzyaloshinskii-Moriya interactions in magnetic properties of graphene derivatives: C_2F and C_2H, Phys. Rev. B **94**, 214411 (2016).

[56] A. A. Mostofi, J. R. Yates, G. Pizzi, Y.-S. Lee, I. Souza, D. Vanderbilt, and N. Marzari, An updated version of WANNIER90: A tool for obtaining maximally-localised Wannier functions. Comput. Phys. Commun. **185**, 2309 (2014).

[57] N. Marzari, A. A. Mostofi, J. R. Yates, I. Souza, and D. Vanderbilt, Maximally localized Wannier functions: Theory and applications, Rev. Mod. Phys. **84**, 1419 (2012).

[58] G. Li, A. E. Antipov, A. N. Rubtsov, S. Kirchner, and W. Hanke, Competing phases of the Hubbard model on a triangular lattice: Insights from the entropy, Phys. Rev. B **89**, 161118(R) (2014).

[59] P. Sahebsara and D. Sénéchal, Hubbard Model on the Triangular Lattice: Spiral Order and Spin Liquid, Phys. Rev. Lett. **100**, 136402 (2008).

[60] P. W. Anderson, New approach to the theory of superexchange interactions, Phys. Rev. **115**, 2 (1959).

[61] J. P. Perdew and A. Zunger, Self-interaction correction to density-functional approximations for many-electron systems, Phys. Rev. B **23**, 5048 (1981).

[62] K. Binder, The Monte Carlo method for the study of phase transitions: A review of some recent progress, J. Comput. Phys. **59**, 1 (1985).

[63] M. Newman and G. Barkema, *Monte Carlo Methods in Statistical Physics* (Oxford University Press, New York, 1999), Chaps. 1–4.

[64] S. Jiang, L. Li, Z. Wang, K. F. Mak, and J. Shan, Controlling magnetism in 2D CrI_3 by electrostatic doping, Nat. Nanotechnol. **13**, 549 (2018).

[65] B. Huang, G. Clark, D. R. Klein, D. MacNeill, E. Navarro-Moratalla, K. L. Seyler, N. Wilson, M. A. McGuire, D. H. Cobden, D. Xiao *et al.*, Electrical control of 2D magnetism in bilayer CrI_3, Nat. Nanotechnol. **13**, 544 (2018).

[66] T. Inoshita, S. Jeong, N. Hamada, and H. Hosono, Exploration for Two-Dimensional Electrides via Database Screening and *Ab Initio* Calculation, Phys. Rev. X **4**, 031023 (2014).

[67] P. V. Sushko, A. L. Shluger, K. Hayashi, M. Hirano, and H. Hosono, Electron Localization and a Confined Electron Gas in Nanoporous Inorganic Electrides, Phys. Rev. Lett. **91**, 126401 (2003).

[68] H. A. Eick, The lanthanoid (ii) halides: Still a veritable gold mine, J. Less-Common Met. **127**, 7 (1987).

[69] D. I. Badrtdinov and S. A. Nikolaev, Localised magnetism in 2D electrides, J. Mater. Chem. C **8**, 7858 (2020).